Supporting Information

Mechanism of ball milled activated carbon in improving the desalination performance of flow- and fixed- electrode in capacitive deionization desalination

Ge Shen[a,b], Junjun Ma[a,b*], Jianrui Niu[a,b], Ruina Zhang[a,b], Jing Zhang[a,b], Xiaoju Wang[a,b], Jie Liu[a,b], Xiqing Li[a,b], Chun Liu[a,b*],

a College of Environmental Science and Engineering, Hebei University of Science and Technology，Shijiazhuang 050018, China

b Pollution Prevention Biotechnology Laboratory of Hebei Province, Shijiazhuang 050018, China

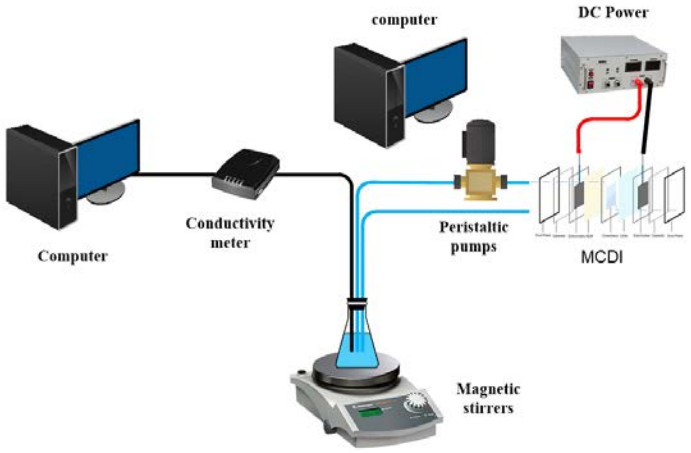

Figure S1 Schematic diagram of the operation of MCDI system

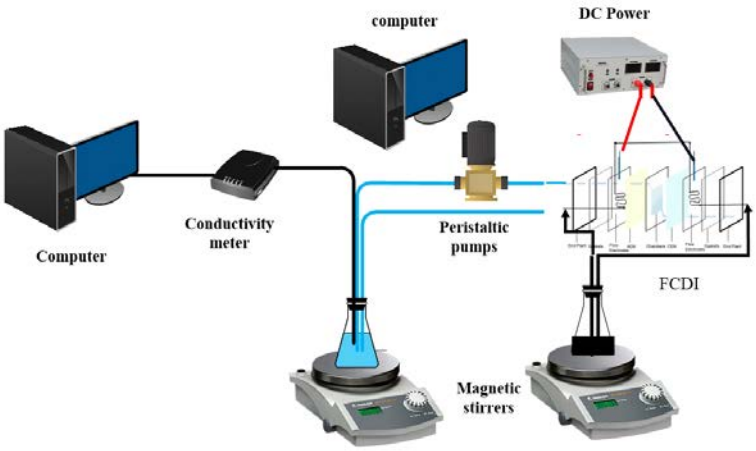

Figure S2 Schematic diagram of the operation of FCDI system

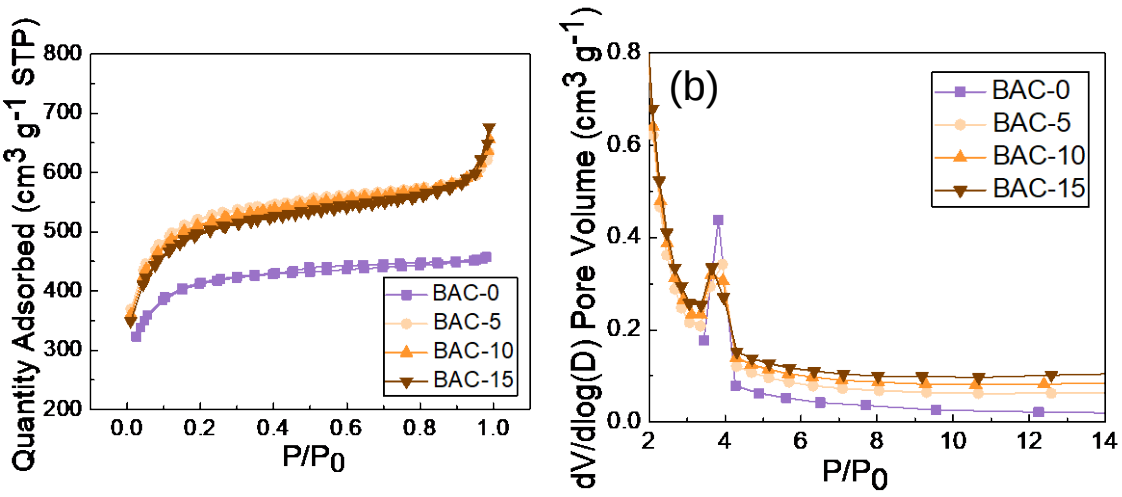

Figure S3 (a) N_2 adsorption−desorption isotherms and (b) the pore-size-distribution curve obtained from the desorption data through the BJH method.

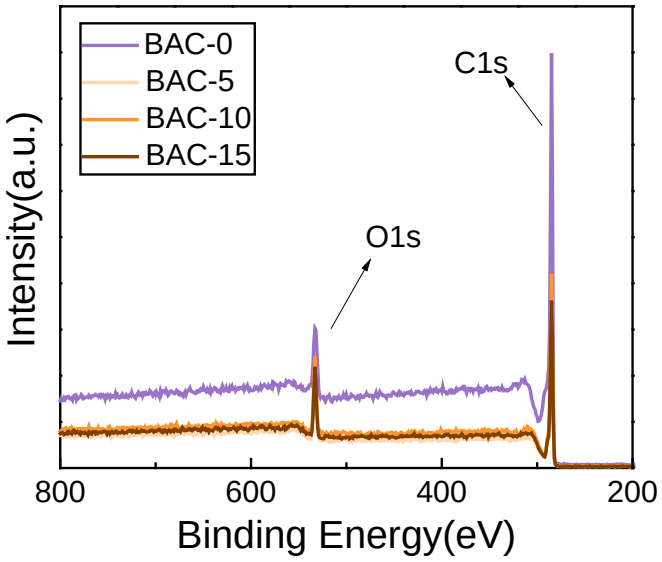

Figure S4 XPS spectra of BACs.

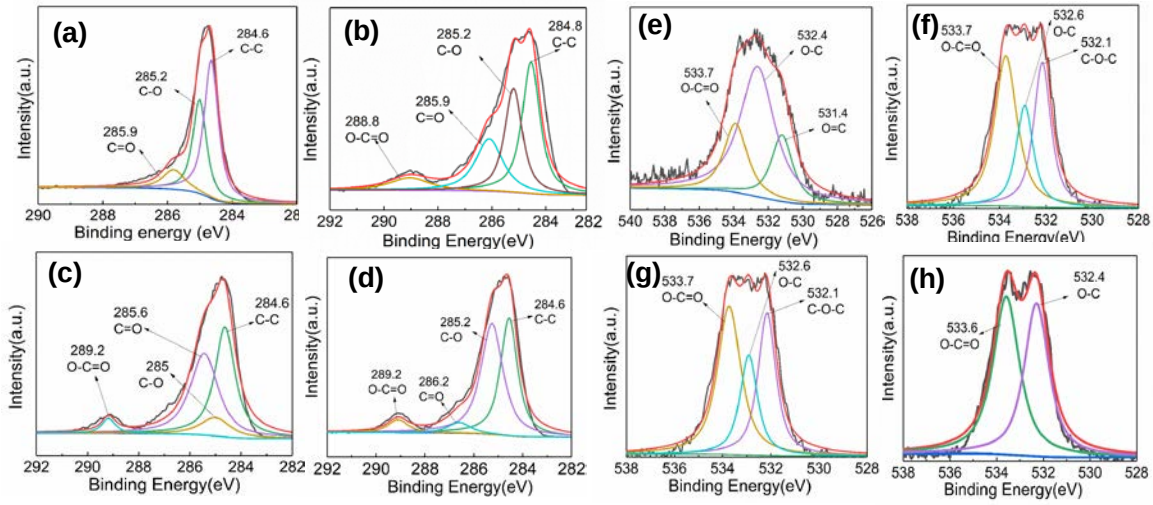

Figure S5. Deconvoluted XPS spectra of C1s（a-d） and O1s (e-h) of BAC-0、BAC-5、BAC-10 and BAC-15 respectively.

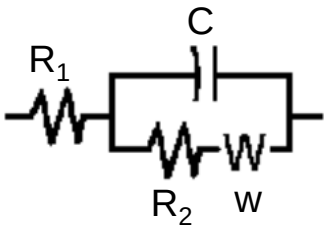

Figure S6. EIS test fitting circuit diagram.

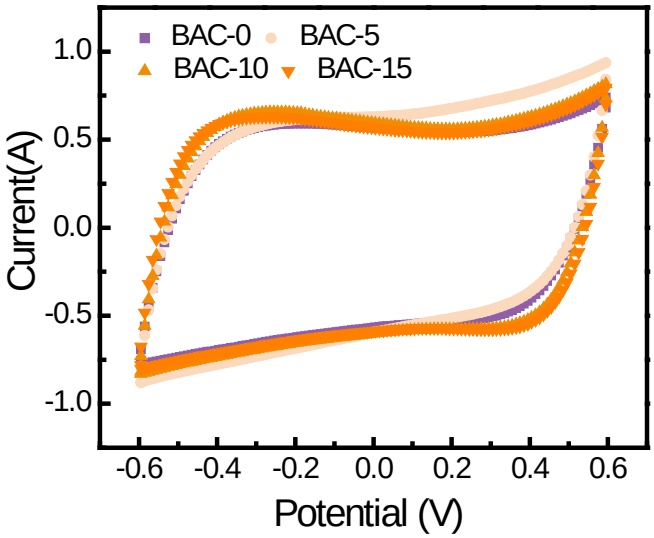

Figure S7. CV curves of BACs.

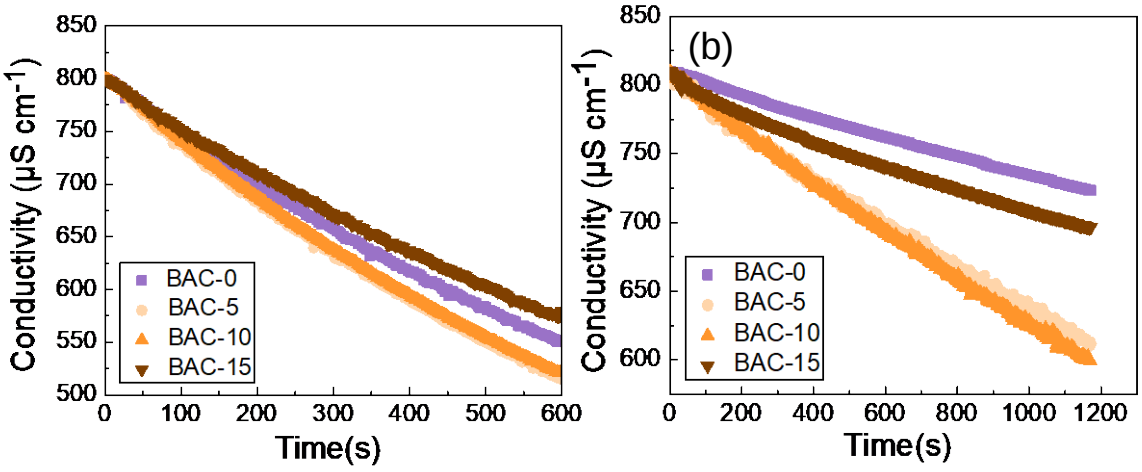

Figure S8 Change of conductivity during desalination process: (a) MCDI; (b) FCDI.

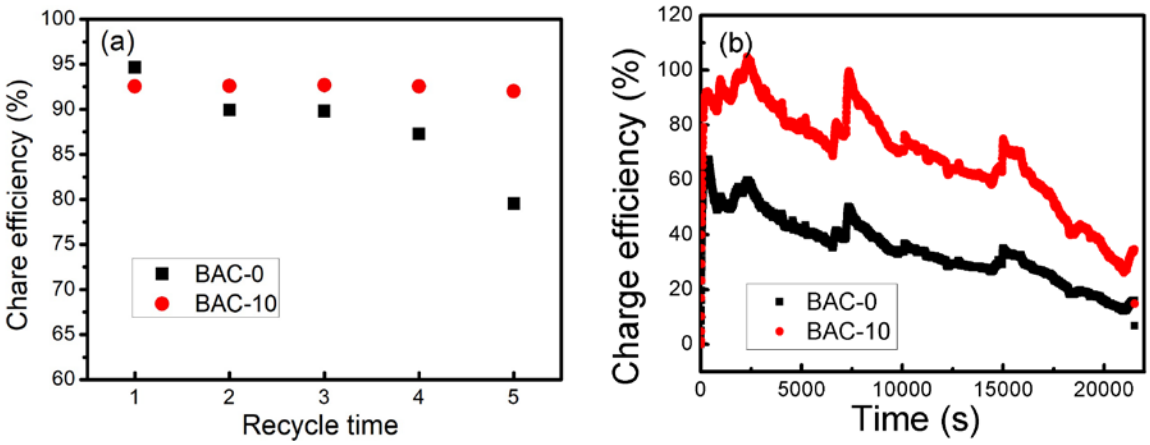

Figure S9 Charge efficiency of AC and BAC in MCDI and FCDI during long desalination, (a) MCDI; (b) FCDI.

Table S1 Electrochemical test results of BACs.

Sample	Capacitance ($F \cdot g^{-1}$)	equivalent resistance (Ω)	Charge transfer resistance (Ω)	equivalent resistance (Ω)	Charge transfer resistance (Ω)
		Fixed electrode		Flow electrode	
BAC-0	39.67	0.82	0.074	41.23	3.00
BAC-5	44.00	0.79	0.035	29.51	2.80
BAC-10	49.33	0.47	0.030	28.01	2.52
BAC-15	43.67	1.01	0.115	38.74	2.81

Table S2 Proportional distribution of groups in the high resolution spectrum of oxygen element

	O-C=O	O-C	O=C	C-O-C
BAC-0	21.1%	60.5%	18.4%	-
BAC-5	35.6%	31.9%	-	32.46%
BAC-10	44.36%	22.6%	-	33.03%
BAC-15	52.8%	47.2%	-	-